Single-Reflection Attenuated Total Reflection of Organic Monolayers on Silicon

M. MILOSEVIC, S. L. BERETS,* and A. Y. FADEEV

Harrick Scientific Corporation, Box 1288, 88 Broadway, Ossining, New York 10562 (M.M., S.L.B.); and Department of Chemistry and Biochemistry, Seton Hall University, 400 South Orange Avenue, South Orange, New Jersey 07079

Index Headings: **Attenuated total reflection; ATR; Internal reflection; Fourier transform infrared spectroscopy; FT-IR; Spectroscopy; Monolayers; Thin films; Grazing angle spectroscopy; Silicon substrates.**

INTRODUCTION

Attenuated total reflection (ATR) spectroscopy, a well-known surface technique, is frequently used for examining very thin films on substrates. However, when it comes to examining thin films on silicon substrates, the high refractive index of the substrates seems to preclude ATR analysis. This paper demonstrates that extraordinary sensitivity can be achieved by using ATR to analyze monolayers on silicon.

THEORY

The theoretical foundations of the ATR technique were provided by Harrick and duPre[1,2] early in the development of ATR as a spectroscopic technique. Harrick and duPre developed formulae for ATR analysis of very thin, weakly absorbing films deposited on a substrate, where the film thickness is much less than the wavelength. When the formulae are applied specifically to the case of a thin film on a silicon substrate, using a Ge ATR crystal and an angle of incidence above the critical, the result exhibits extraordinary sensitivity to thin films. This sensitivity enhancement was seized upon by Olsen and Shimura[3,4] who calculated that, for the case of SiO_2 film on Si wafer and the angle of incidence of 60°, the enhancement was over 100 times per reflection over what would have been measured in transmission. In an attempt to further enhance the sensitivity, they used multiple reflection ATR in their experimental work. The results, while impressive, fall short of exhibiting the enhancement of over 1500 that was predicted by the authors. Olsen and Shimura did not discuss the degree of enhancement; they were content with getting good experimental results. They probably did not achieve the predicted theoretical enhancement due to imperfect contact between the sample and the ATR crystal.

It is relatively straightforward to arrive at the expression for the reflectivity of a thin film sandwiched between two media:[5,6]

$$\rho^p = \frac{r_{12}^p + r_{23}^p e^{4\pi i k d\sqrt{n_2^2 - n_1^2 \sin^2\vartheta}}}{1 + r_{12}^p r_{23}^p e^{4\pi i k d\sqrt{n_2^2 - n_1^2 \sin^2\vartheta}}} \quad (1)$$

where the index p indicates polarization of incident light, r_{12}^p and r_{23}^p are Fresnel amplitude coefficients[6] for the interface between media (layers 1 and 3) and the film (layer 2), k is the wavenumber ($k = 1/\lambda$), and ϑ is the angle of incidence of incident radiation. The refractive indices of the media could be complex to allow applicability of Eq. 1 for the case of absorbing media. The expression in Eq. 1 is the ratio of reflected and incident electric-field amplitudes. This expression describes the magnitude of the reflected electric field and the phase shift of the reflected field with respect to the incident field. The square of the absolute value of the amplitude coefficient (see Eq. 1) is the theoretical quantity to be compared to measured reflectance.

Now, consider the case where the film is sandwiched between a germanium ATR crystal (n_1) and a silicon wafer (n_3). Below the critical angle, the electromagnetic wave refracts into the film, propagates to the film–silicon interface, partially reflects from that interface (some light is refracted into the silicon), propagates back to the germanium ATR element, partially reflects from the germanium–film interface, and so on (as shown in Fig. 1). Within the film, electric-field vectors of all of the partially reflected waves add. The resulting electric field is an infinite sum of the contributions from all of the reflected waves. This structure of the infinite sum of all the multiply reflected waves is reflected in Eq. 1.

Equation 1 can be expanded using a Taylor series, taking advantage of the following identities: $r_{n,n+1}r_{n+1,n} + t_{n,n+1}t_{n+1,n} = 1$, $r_{n,n+1} = -r_{n+1,n}$. Introducing the shorthand notation, $z = e^{2\pi i k d\sqrt{n_2^2 - n_1^2 \sin^2\vartheta}}$, and dropping the polarization index p gives:

$$\begin{aligned}\rho &= \frac{r_{12} + r_{23}z^2}{1 + r_{12}r_{23}z^2} \\ &= r_{12} + t_{12}t_{21}z(zr_{23}) + t_{12}t_{21}z(zr_{23})^2(zr_{21}) \\ &\quad + t_{12}t_{21}z(zr_{23})^3(zr_{21})^2 + \cdots \end{aligned} \quad (2)$$

The terms in the above sum can be related to the components of the reflected wave in a direct one-to-one fashion.

The first term is just the reflection coefficient of the interface between materials 1 and 2, corresponding to R1 in Fig. 1. The second term corresponds to the ray R2 in Fig. 1, and all the following terms correspond to the subsequent reflections. Thus, there is a strict geometric representation of the terms in the Taylor series (see Eq. 2). Since this is just another expression of Eq. 1, the geometrical representation can continue to be relied upon both in the subcritical and supercritical incident angle regimes.

Above the critical angle for this system, the electromagnetic wave beyond the totally internally reflecting interface is evanescent. This means that the wave propagates parallel to the interface. Hence, the evanescent wave cannot reflect from the film–silicon interface. However, each term in the infinite sum remains meaningful. Since the reflectance amplitude coefficients be-

Received 12 August 2002; accepted 31 January 2003.
* Author to whom correspondence should be sent.

0003-7028/03/5706-0724$2.00/0

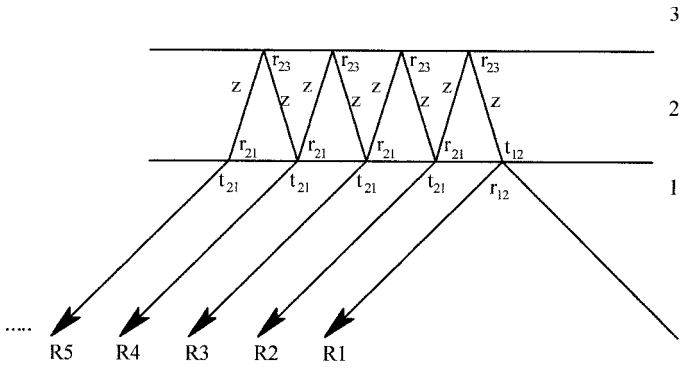

FIG. 1. Multiple reflections in the sample layer.

come of unit amplitude above the critical angle, the higher terms in Eq. 2 become more significant. For very thin films, the phase-shifts between the components are negligible and the contributions to the electric-field component perpendicular to the interface of all terms become constructive. This greatly enhances the electric-field strength within the film. Since the absorption is proportional to the square of the electric-field amplitude, an enhancement in the electric-field strength of ten times results in a hundredfold enhancement in absorption.

EXPERIMENTAL

Numerical simulations and experimental measurements were carried out to demonstrate this extraordinary sensitivity. Both used a germanium ATR crystal slightly above the critical angle to study an organic thin film on a silicon substrate.

For the numerical analysis, the experimental parameters were selected as follows:

$n_1 = 4.0$	(germanium ATR crystal)
$n_2 = 1.5 + 0.5i$	(sample)
$n_3 = 3.45$	(silicon substrate)
$k = 1000\ \text{cm}^{-1}$	(wavenumber of incident light, $\lambda = 10\ \mu\text{m}$)
$d = 1$ nm	(10 Å)
$\theta = 60°$	

Note that a typical organic sample has the real part of the refractive index around 1.5; hence the above choice. The value of the imaginary part of the refractive index (i.e., absorption index, κ) of the sample is chosen to correspond to the center of a fairly strong absorption band. To get a sense of the strength of the absorption index chosen and thus be able to correlate the simulated results to actual samples, one can calculate the absorbance that would be measured for this peak in a transmission measurement with a pathlength of $d = 10\ \mu$m. If the peak were located in the carbonyl region ($k \approx 1700\ \text{cm}^{-1}$), the absorbance measured would be (neglecting the reflectance losses):

$$A = 0.434 \times 4\pi k\kappa d = 4.6$$

This is a rather strong absorber, as stated above. The results of the numerical simulation using these parameters are presented graphically.

The supported organic monolayers were prepared by the reaction of $ClSi(CH_3)_2(CH_2)_3Si[OSi(CH_3)_3]_3$, further silane, with Si wafers (International Wafer Service, (100) orientation, P/B doped, resistivity from 20 to 40 ohm-cm, thickness ~450–575 μm) according to the following scheme:

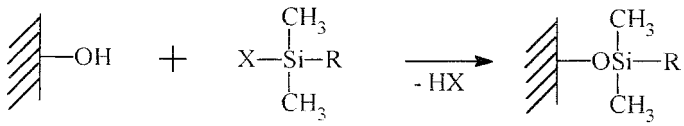

X=Cl; R=$(CH_2)_3Si[OSi(CH_3)_3]_3$

The reaction procedure was similar to that published in earlier work.[7] Briefly, the synthesis included the following steps. Prior to the reaction with silane, Si wafers were cleaned using a freshly prepared solution made from seven parts of concentrated sulfuric acid, dissolved sodium dichromate (~3–5 wt %), and three parts of 30% hydrogen peroxide. The Si wafers were submerged in this cleaning solution overnight, rinsed with five to seven 50 mL aliquots of water, and placed in a clean oven at 120 °C for 1–2 h. The dried Si plates were covered with anhydrous toluene (5–10 mL) containing ethyldiisopropylamine (10^{-3} M). Then 0.5 mL of silane was added by syringe and the reaction mixture was left at room temperature for 3 days. The wafers were isolated and rinsed sequentially with 2 × 10 mL of toluene, 3 × 10 mL of ethanol, 2 × 10 mL of an ethanol–water mix (1:1), 2 × 10 mL of water, 2 × 10 mL of ethanol, and 2 × 10 mL of water. After rinsing, the wafers were dried in a clean oven at 120 °C for 10 min.

Ellipsometric characterization of bare Si wafers and Si-supported monolayers were made with an Inomteck Automatic Ellipsometer. The light source was a He–Ne laser with $\lambda = 632.8$ nm. The angle of incidence was 70°. Measurements were performed for 3–5 different spots on the sample. The thickness of the layer was calculated from the ellipsometric parameters (Δ and Ψ) using the Inomteck software. The thickness of the silicon oxide overlayer on the Si substrate was calculated using the following settings: single-layer model, air: $n_0 = 1$; silicon oxide layer: $n_2 = 1.462$; silicon substrate: $n_S = 3.858 + 0.018i$. The thickness of silicon oxide for the bare Si wafers was 2.1 ± 0.05 nm after the cleaning. For the Si supported monolayers, the calculations were performed for the transparent double-layer model (silicon substrate/silicon oxide/alkylsilane layer/air) with the following parameters: air: $n_0 = 1$; alkylsilane layer: $n_1 = 1.45$; silicon oxide layer: $n_2 = 1.462$ (the thickness of this oxide layer was fixed at 2.1 nm); silicon substrate: $n_S = 3.858 + 0.018i$. The thickness of the monolayer was obtained as 0.9 ± 0.1 nm.

The ATR measurements were carried out using Harrick's Seagull™[8] variable angle reflection accessory used in conjunction with a Bruker Vector 22 spectrometer. A spectrum was collected with 32 scans, an 8 cm^{-1} resolution, and a 65° incident angle. Note that the experimental apparatus focuses the beam onto the sample

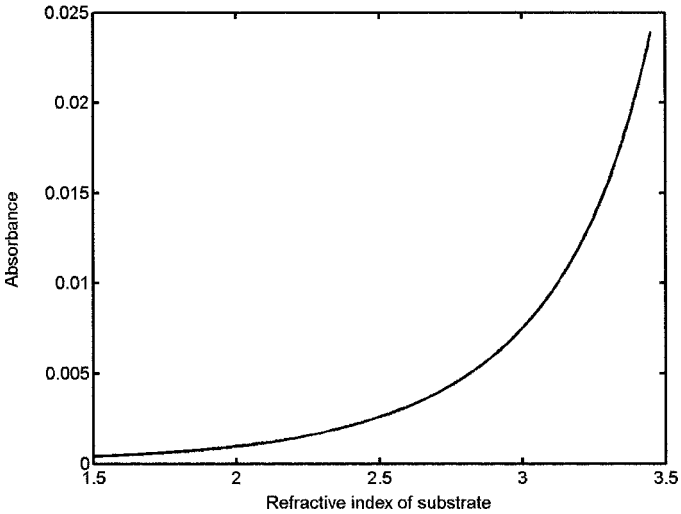

FIG. 2. Absorbance of a thin film shown as a function of the refractive index of the substrate.

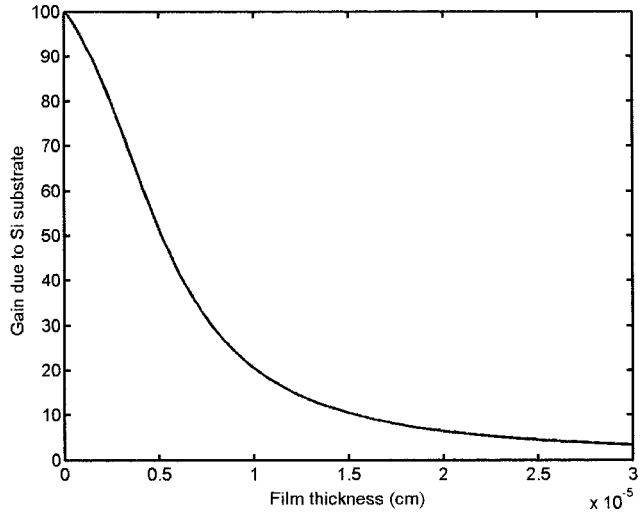

FIG. 4. The enhancement of absorbance due to the silicon substrate vs. thickness.

and hence supplies a range of incident angles, as opposed to the collimated beam assumed by the theoretical model. To avoid contributions from rays below the critical angle, the experimental incident angle was chosen to be slightly higher than the angle used in the simulations.

The coated Si wafers were cut to fit into the ATR holder of the Seagull™. A special pressure applicator was used to optimize contact between the sample and the ATR crystal.

RESULTS AND DISCUSSION

The results of the numerical analysis are shown in Figs. 2 through 4. Figure 2 shows the intriguing dependence of the measured absorbance of the thin film on the refractive index of the substrate. The angle of incidence was kept constant at 60° and the absorption index of the film at 0.5. The change in the refractive index of the substrate is between that of the thin film (1.5) and the silicon wafer (3.45). The increase in sensitivity is remarkable. This clearly shows that the high refractive index of the substrate is the crucial ingredient leading to the increased sensitivity.

In Fig. 3, the film thickness increased from 10 Å to 1 μm. It is most intriguing to see that the measured absorbance of the film first dramatically increases, reaching a maximum for film thickness of around 400 Å. After that, the absorbance dramatically decreases, although more sample (thicker film) is being added into the evanescent wave and hence a greater proportion of the evanescent wave could be absorbed. The absorbance decrease after 400 Å is indicative of the decreasing electric-field strength of the evanescent wave, and that decrease dominates over the increase in film thickness.

If the silicon substrate were not present, the increase in film thickness would lead to increase in absorbance. For very thin films, compared to the wavelength of light, the absorbance and film thickness are proportional. As the film thickness reaches the penetration depth, the linear relationship becomes saturated, and further increases in film thickness bring no increase in measured absorbance. The absorbance never decreases with increases in film thickness. This is what makes this case very interesting both from the theoretical and practical points of view.

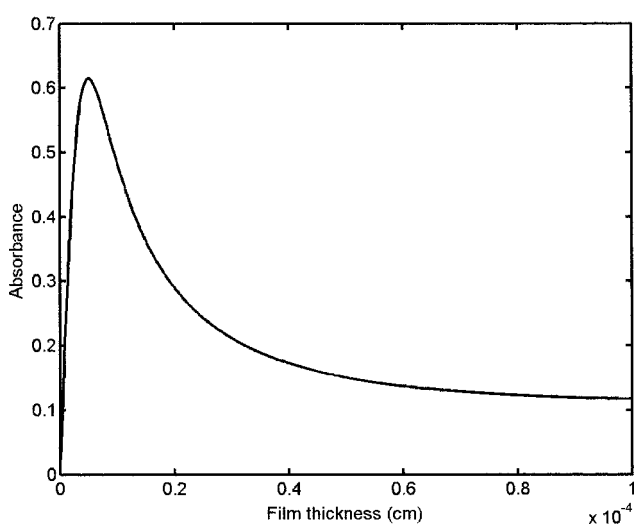

FIG. 3. Absorbance vs. film thickness.

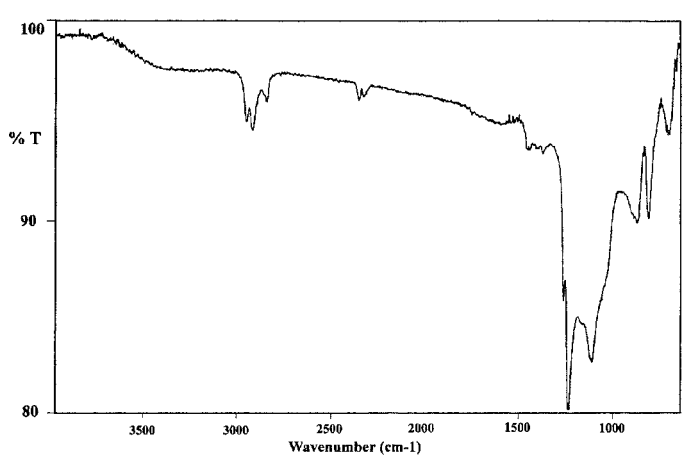

FIG. 5. ATR spectrum of an organic monolayer on a silicon wafer.

Next, the level of enhancement as a function of film thickness was calculated for the case where film is on a silicon substrate relative to the case where no substrate is present. The result is shown in Fig. 4.

Although the absorbance, as a function of film thickness, exhibits a sharp maximum (Fig. 3), the enhancement in sensitivity is a monotonically decreasing function of film thickness. For very thin films, the enhancement is roughly a factor of one hundred. Thus, the method is the most sensitive for the thinnest films, just where the sensitivity is most needed.

Figure 5 shows an experimental spectrum of an organosilane monolayer supported on a Si wafer. The absorbance bands are consistent with the structure of the organosilane used for the monolayer synthesis: ~2960–2850 cm^{-1} (CH stretching), ~1260 cm^{-1} (Si–CH_3), and 1100 cm^{-1} (Si–O). Note that the spectrum exhibits extremely strong absorbance levels considering that the monolayer is only 0.9 nm thick according to ellipsometry.

CONCLUSION

Grazing angle ATR has extraordinarily high sensitivity for analyzing thin films on silicon substrates by infrared spectroscopy. For samples with stable monolayers and coatings, this method is far superior to those currently in use. Additional work is in progress to further refine the physical picture underlying this extraordinary sensitivity and to apply this technique to thin films on metal substrates.

1. N. J. Harrick and F. K. duPre, Appl. Opt. **5,** 1739 (1966).
2. N. J. Harrick, *Internal Reflection Spectroscopy* (John Wiley and Sons, New York, 1967).
3. J. E. Olsen and F. Shimura, Appl. Phys. Lett. **53,** 1934 (1988).
4. J. E. Olsen and F. Shimura, J. Appl. Phys. **66,** 1353 (1989).
5. M. Born and E. Wolf, *Principles of Optics* (University Press, Cambridge, UK, 1999).
6. M. Milosevic and S. L. Berets, Appl. Spectrosc. **47,** 566 (1993).
7. A. Y. Fadeev and T. J. McCarthy, Langmuir **15,** 3759 (1999).
8. M. Milosevic, N. J. Harrick, and S. L. Berets, Appl. Spectrosc. **45,** 126 (1991).